Inorg. Chem. **2003**, *42*, 5909–5916

Redox Interplay of Oxo–Thio–Tungsten Centers with Sulfur-Donor Co-Ligands

Simon Thomas,[1a] Aston A. Eagle,[1a] Stephen A. Sproules,[1a] Jason P. Hill,[1a] Jonathan M. White,[1a] Edward R. T. Tiekink,[1b] Graham N. George,[1c] and Charles G. Young*,[1a]

School of Chemistry, University of Melbourne, Victoria 3010, Australia, Department of Chemistry, University of Adelaide, Adelaide, South Australia 5005, Australia, and Stanford Synchrotron Radiation Laboratory, SLAC, Stanford University, P.O. Box 4349, MS 69, Stanford, California 94309

Received March 13, 2003

The oxo–thio–W(VI) complexes Tp*WOS(S_2PR_2-*S*) and Tp*WOS(pyS-*S*) (Tp* = hydrotris(3,5-dimethylpyrazol-1-yl)borate, R = OEt, Ph; pyS = pyridine-2-thiolate) have been prepared and characterized by microanalytical, spectroscopic, and structural techniques. Crystals of the 1,2-dichloroethane hemisolvate of Tp*WOS(S_2PPh_2-*S*) belong to the triclinic space group $P\bar{1}$ with $a = 10.732(6)$ Å, $b = 16.91(1)$ Å, $c = 10.021(4)$ Å, $\alpha = 104.40(4)°$, $\beta = 107.52(3)°$, $\gamma = 96.09(5)°$, $V = 1647(1)$ Å^3 for $Z = 2$. The complex exhibits a distorted octahedral structure featuring a facial tridentate Tp* ligand and mutually *cis* terminal oxo (W–O(1) = 1.712(7) Å), terminal thio (W–S(1) = 2.162(3) Å), and monodentate dithiophosphinate ligands. X-ray absorption and extended X-ray absorption fine structure results support a related oxo–thio formulation for Tp*WOS(pyS-*S*). The complexes are reduced to the corresponding oxo–thio–W(V) anions, $[Tp^*WOS(S_2PR_2\text{-}S)]^-$ and $[Tp^*WOS(pyS\text{-}S)]^-$, which exhibit highly anisotropic EPR spectra. They are oxidized to form the EPR-active (dithio)oxo–W(V) cations, $[Tp^*WO(S_3PR_2\text{-}S,S')]^+$ and $[Tp^*WO(pyS_2\text{-}N,S)]^+$ (pyS_2 = pyridine-2-dithio). Green $[Tp^*WO(pyS_2\text{-}N,S)]BF_4$, formed in the reaction of Tp*WOS(pyS) and $NOBF_4$, has been isolated and spectroscopically and structurally characterized. Crystals of $[Tp^*WO(pyS_2\text{-}N,S)]BF_4$ belong to the monoclinic space group *Cc* with $a = 16.007(5)$ Å, $b = 14.091(4)$ Å, $c = 13.608(4)$ Å, $\beta = 124.525(4)°$, $V = 2528.8(13)$ Å^3 for $Z = 4$. The cation exhibits a distorted octahedral structure featuring facial tridentate Tp*, terminal oxo (W–O(1) = 1.632(12) Å), and bidentate pyridine-2-dithio-*N*,*S* (W–S(1) = 2.317(7) Å, S(1)–S(2) = 2.037(9) Å) ligands. The structures and redox behavior of the complexes are compared and contrasted with those of the related molybdenum complexes, $Tp^*Mo^{VI}OS(S_2PR_2\text{-}S)$ and $Tp^*Mo^{IV}O(pyS_2\text{-}N,S)$ (Hill, J. P.; Laughlin, L. J.; Gable, R. W.; Young, C. G. *Inorg. Chem.* **1996**, *35*, 3447).

Introduction

Metal−sulfur compounds have important technological applications and are employed as catalysts for many industrial processes.[2,3] Moreover, metal−sulfur centers play vital roles in biological electron transport and enzyme-catalyzed reactions.[3,4] Redox processes involving the metal center(s) and sulfur, acting alone or in concert, are essential for many of these applications. The potential for M/S redox interplay in these systems is underscored by often unpredictable outcomes, including multisite redox changes and facile ligand transformations, in "simple" reactions involving metal thio(late) complexes;[2−5] induced internal redox reactions are among the most striking and well-defined reactions of this type.[6]

In previous work,[7] we compared the molecular and electronic structures of the complexes $Tp^*Mo^{VI}OS(S_2PPr^i_2\text{-}S)$[8] and $Tp^*Mo^{IV}O(pyS_2\text{-}N,S)$ (Tp* = hydrotris(3,5-dimethylpyrazol-1-yl)borate, pyS_2 = pyridine-2-dithio). The spectroscopic and structural properties of these complexes,

(1) (a) University of Melbourne. (b) University of Adelaide. Present address: Department of Chemistry, National University of Singapore, Singapore 117543. (c) Stanford University.
(2) Stiefel, E. I. In *Kirk-Othmer Encyclopedia of Chemical Technology*, 4th ed.; Wiley: New York, 1995; Vol. 16, p 940.
(3) *Sulfur, Its Significance for Chemistry, for the Geo-, Bio-, and Cosmosphere and Technology*; Müller, A., Krebs, B., Eds.; Elsevier: Amsterdam, 1984.
(4) *Transition Metal Sulfur Chemistry*; Stiefel, E. I., Matsumoto, K., Eds.; ACS Symposium Series 653, American Chemical Society: Washington, DC, 1996.
(5) Stiefel, E. I. *J. Chem. Soc., Dalton Trans.* **1997**, 3915.

10.1021/ic030095g CCC: $25.00
Published on Web 08/28/2003

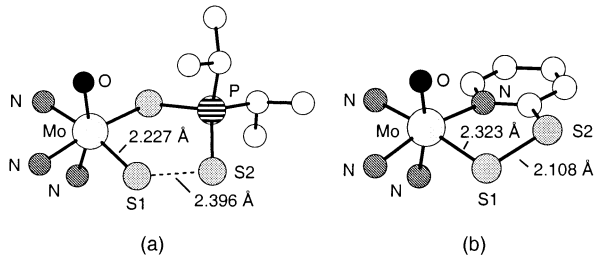

Figure 1. (a) Partial structure of Tp*MoOS($S_2PPr^i_2$). (b) Partial structure of Tp*MoO(pyS_2). Only the three N donor atoms of Tp* are shown.

Chart 1

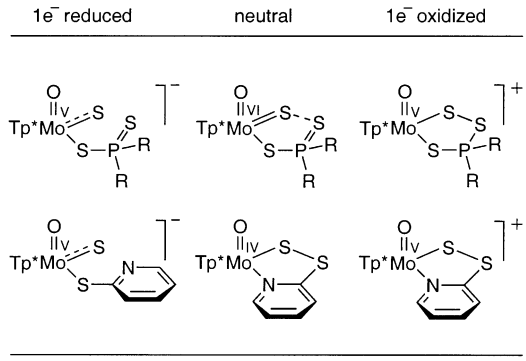

particularly the observed Mo−S(1) and S(1)−S(2) distances (Figure 1), were consistent with oxo−thio−Mo(VI) and (dithio)oxo−Mo(IV) formulations, respectively. The generation of Mo(V) species upon reduction or oxidation of these complexes (Chart 1) provided an elegant demonstration of the redox versatility of Mo−S centers and induced internal redox reactions.[7] In other work, we have compared the electrochemical properties of oxo− and thio−Mo and −W complexes.[9−12] Dioxo− and oxo−thio−W complexes are more difficult to reduce than their Mo and/or bis(thio)−W counterparts; consequently, thio−W complexes are generally more stable than thio−Mo species. Very recently, we described a mononuclear oxo−thio−Mo(VI) complex, Tp^{Pr}-MoOS(OPh) (Tp^{Pr} = hydrotris(3-isopropylpyrazol-1-yl)-borate), that participates in a delicately poised redox equilibrium with the dimeric μ-disulfido−Mo(V) complex, $[Tp^{Pr}MoO(OPh)]_2(\mu\text{-}S_2)$.[13] Consistent with the outcomes of electrochemical studies, there is no evidence of similar reactions in related oxo−thio−W(VI) systems (vide infra).[10−12]

In light of the contrasting redox interplay of S with Mo and W and the enhanced stability of thio−W(VI) versus thio−Mo(VI) complexes, we have examined the structural, electronic, and redox properties of the W "analogues" of Tp*MoOS($S_2PPr^i_2$) and Tp*MoO(pyS_2). Accordingly, this paper reports the synthesis and characterization of the oxo−thio−W(VI) complexes, $Tp^*W^{VI}OS(S_2PR_2\text{-}S)$ and $Tp^*W^{VI}OS(pyS\text{-}S)$ (pyS = pyridine-2-thiolate), and aspects of their redox chemistry. The W complexes are less susceptible to reduction than the Mo complexes and are stable in the absence of M=S···S interactions. However, as with the Mo complexes, they undergo reduction or oxidation to produce W(V) species via direct or induced internal redox reactions.

Experimental Section

Materials and Methods. Reactions were performed under anaerobic conditions using dried and distilled solvents and standard Schlenk line techniques. Samples of Tp*WS{$S_2P(OEt)_2$}(CO),[14] Tp*WS(S_2PPh_2)(CO),[14] and Tp*WOSCl[12] were prepared according to published procedures. Sodium pyridine-2-thiolate was prepared by refluxing a mixture of pyridine-2-thiol (1.0 g, 9 mmol) and sodium (0.21 g, 9 mmol) in toluene (25 mL) for 2 h under dinitrogen. The white solid produced was isolated by filtration and dried under vacuum.

Infrared spectra were recorded on a Perkin-Elmer 1430 spectrophotometer as pressed KBr disks. Proton NMR spectra were obtained using a Varian FT Unity-300 spectrometer and were referenced to internal $CHCl_3$ (δ_H 7.23). EPR spectra were recorded on a Bruker FT ECS-106 spectrometer using 1,1-diphenyl-2-picrylhydrazyl as reference. Electronic spectra were obtained on Shimadzu UV-240 and Hitachi 150-20 UV spectrophotometers. Electrochemical experiments were performed using a Cypress electrochemical system II with a 3 mm glassy carbon working electrode and platinum auxiliary and reference electrodes. Solutions of the complexes (1−2 mM) in 0.1 M NBu_4BF_4/acetonitrile were employed, and potentials were referenced to internal ferrocene ($E_{1/2}$ = +0.390 V vs SCE). Potentials are reported relative to the saturated calomel electrode (SCE). Mass spectra were recorded on a Vacuum Generators VG ZAB 2HF mass spectrometer. Microanalyses were performed by Atlantic Microlabs, Norcross, GA.

Syntheses. Tp*WOS{$S_2P(OEt)_2$}. A solution of Tp*WS{$S_2P(OEt)_2$}(CO) (1.20 g, 1.65 mmol) and pyridine *N*-oxide (0.38 g, 4.00 mmol) in toluene (40 mL) was heated at reflux for 24 h. The reaction mixture was then reduced to dryness, and the residue was column chromatographed using silica gel/dichloromethane to yield an orange fraction. The product was recrystallized from dichloromethane/methanol as orange crystals which were filtered, washed with methanol (5 mL), and dried in vacuo. Yield: 0.73 g, 62%.

Anal. Calcd for $C_{19}H_{32}BN_6O_3PS_3W$: C, 31.95; H, 4.52; N, 11.77; S, 13.46. Found: C, 32.06; H, 4.55; N, 11.84; S, 13.37. IR (KBr): 2980 m, 2930 m, ν(BH) 2554 m, ν(CN) 1543 s, 1446 s, 1415 s,

(6) Induced internal electron transfer reactions involving Mo(VI) and W(VI) include the following: (a) Pan, W.-H.; Harmer, M. A.; Halbert, T. R.; Stiefel, E. I. *J. Am. Chem. Soc.* **1984**, *106*, 459. (b) Pan, W.-H.; Halbert, T. R.; Hutchings, L. L.; Stiefel, E. I. *J. Chem. Soc., Chem. Commun.* **1985**, 927. (c) Harmer, M. A.; Halbert, T. R.; Pan, W.-H.; Coyle, C. L.; Cohen, S. A.; Stiefel, E. I. *Polyhedron* **1986**, *5*, 341. (d) Sarkar, S.; Ansari, M. A. *J. Chem. Soc., Chem. Commun.* **1986**, 324. (e) Ansari, M. A.; Chandrasekaran, J.; Sarkar, S. *Inorg. Chem.* **1988**, *27*, 763. (f) Coyle, C. L.; Harmer, M. A.; George, G. N.; Daage, M.; Stiefel, E. I. *Inorg. Chem.* **1990**, *29*, 14. (g) Gea, Y.; Greaney, M. A.; Coyle, C. L.; Stiefel, E. I. *J. Chem. Soc., Chem. Commun.* **1992**, 160. (h) Wang, K.; McConnachie, J. M.; Stiefel, E. I. *Inorg. Chem.* **1999**, *38*, 4334.

(7) Hill, J. P.; Laughlin, L. J.; Gable, R. W.; Young, C. G. *Inorg. Chem.* **1996**, *35*, 3447. In this and related papers, the abbreviation L was employed for the Tp* ligand.

(8) Eagle, A. A.; Laughlin, L. J.; Young, C. G.; Tiekink, E. R. T. *J. Am. Chem. Soc.* **1992**, *114*, 9195.

(9) Eagle, A. A.; Tiekink, E. R. T.; Young, C. G. *Inorg. Chem.* **1997**, *36*, 6315.

(10) Eagle, A. A.; Harben, S. M.; Tiekink, E. R. T.; Young, C. G. *J. Am. Chem. Soc.* **1994**, *116*, 9749.

(11) (a) Eagle, A. A.; Thomas, S.; Young, C. G. In *Transition Metal Sulfur Chemistry: Biological and Industrial Significance*; Stiefel, E. I., Matsumoto, K., Eds.; ACS Symposium Series No. 653; American Chemical Society: Washington, DC, 1996; pp 324−335. (b) Thomas, S.; Tiekink, E. R. T.; Young, C. G. *Organometallics* **1996**, *15*, 2428.

(12) Eagle, A. A.; Tiekink, E. R. T.; George, G. N.; Young, C. G. *Inorg. Chem.* **2001**, *40*, 4563.

(13) Smith, P. D.; Slizys, D. A.; George, G. N.; Young, C. G. *J. Am. Chem. Soc.* **2000**, *122*, 2946.

(14) Thomas, S. Ph.D. Dissertation, University of Melbourne, 1997.

1383 m, 1358 s, 1212 s, 1070 s, 1039 s, 1018 s, ν(P−O_{alkyl}) 951, ν(W═O) 931, 859 w, 812 w, 786 m, ν(P═S) 659 or 646 s, ν(P−S) 533 m, ν(W═S) 488 m cm^{-1}. ^1H NMR ($CDCl_3$): δ 1.37 (t, 3H, ^3J = 7.0 Hz, −CH_2CH_3), 1.41 (t, 3H, ^3J = 6.9 Hz, −CH_2CH_3), 2.35, 2.38, 2.39, 2.65, 2.69, 2.90 (each s, 3H each, 6 CH_3 of Tp*), 4.25 (m, 2H, −CH_2CH_3), 4.42 (m, 2H, −CH_2CH_3), 5.85, 5.94, 5.96 (each s, 1H each, 3 CH of Tp*). $^{31}P\{^1H\}$ NMR ($CDCl_3$): δ 121.42. Mass spectrum, *m*/*z*: 713 $[M - H]^+$. Electronic spectrum (CH_2Cl_2): 490 (160), 400 nm (ϵ 2360 $M^{-1}\cdot cm^{-1}$).

Tp*WOS(S_2PPh_2). A solution of Tp*WS(S_2PPh_2)(CO) (0.82 g, 1.04 mmol) and pyridine *N*-oxide (0.40 g, 4.21 mmol) in toluene (60 mL) was heated at reflux for 48 h. The reaction mixture was then reduced to dryness, and the residue was column chromatographed using silica gel/dichloromethane to yield an orange fraction. The product was recrystallized from dichloromethane/methanol as orange crystals which were filtered, washed with methanol (5 mL), and dried in vacuo. Yield: 0.32 g, 38%.

Anal. Calcd for $C_{27}H_{32}BN_6OPS_3W\cdot 0.5CH_2Cl_2$: C, 40.24; H, 4.05; N, 10.24; S, 11.72. Found: C, 40.04; H, 4.06; N, 10.15; S, 12.06. IR (KBr): 2961 w, 2853 w, ν(BH) 2555 m, ν(CN) 1544 s, 1480 w, ν(Ph) 1450 s, 1437 s, 1415 s, 1384 s, 1360 s, 1308 w, 1211 s, 1187 m, 1097 s, 1074 s, 1041 s, 999 w, ν(W═O) 931 s, 909 w, 876 w, 860 s, 815 m, 792 m, 744 m, 709 s, 690 s, ν(P═S) 643 s, 614 m, ν(P−S) 525 s, ν(W═S) 485 s, 474 s cm^{-1}. ^1H NMR ($CDCl_3$): δ 2.35, 2.36, 2.38, 2.51, 2.54, 2.66 (each s, 3H each, 6 CH_3 of Tp*), 5.80, 5.85, 5.95 (each s, 1H each, 3 CH of Tp*), 7.41, 7.92, 8.13 (each m, total 10H, 2 Ph). $^{31}P\{^1H\}$ NMR ($CDCl_3$): δ 67.71. Mass spectrum, *m*/*z*: 777 $[M - H]^+$. Electronic spectrum (CH_2Cl_2): 475 (40), 395 nm (ϵ 5520 $M^{-1}\cdot cm^{-1}$).

Tp*WOS(pyS). A mixture of Tp*WOSCl (150 mg, 0.31 mmol), sodium 2-pyridine thiolate (35 mg, 0.31 mmol), and 18-crown-6 (∼5 mg) was refluxed in toluene (20 mL) for 1 h. A color change from pink to orange was observed, and at the end of the reaction, one major product at low R_f was detectable by thin-layer chromatography (silica, CH_2Cl_2). The solvent was removed, and the residue was dissolved in CH_2Cl_2 and column chromatographed on silica gel using 4/1 CH_2Cl_2−CH_3CN as eluent. The main orange band was collected and evaporated. The residue was recrystallized from CH_2Cl_2/hexanes to yield red crystals. Yield: 130 mg, 66%.

Anal. Calcd for $C_{20}H_{26}BN_7OS_2W$: C, 37.58; H, 4.10; N, 15.34; S, 10.03. Found: C, 37.33; H, 4.16; N, 15.16; S, 9.83. IR (KBr): ν(BH) 2546 m, 1575 m, ν(CN) 1544 s, 1493 w, 1448 s, 1413 s, 1382 m, 1364 s, 1270 w, 1211 s, 1187 m, 1148 w, 1111 w, 1068 s, 1040 m, 988 w, ν(W═O) 923 s, 857 m, 815 m, 795 m, 757 s, 713 m, 693 s, 647 m, ν(W═S) 480 m cm^{-1}. ^1H NMR ($CDCl_3$): δ 2.38, 2.39 (6H), 2.62, 2.67, 2.74 (each s, 3H unless stated, 6 CH_3 of Tp*), 5.87, 5.88, 5.98 (each s, 1H each, 3 CH of Tp*), 7.02, 7.63 (each t, 1H, py), 8.10, 8.59 (each d, 1H, py). Mass spectrum, *m*/*z*: 639 $[M]^+$.

[Tp*WO(pyS_2)]BF_4. A mixture of Tp*WOS(pyS) (100 mg, 0.16 mmol) and $NOBF_4$ (19 mg, 0.16 mmol) was treated with CH_2Cl_2 (20 mL), and the mixture was stirred. A color change from orange to bright green was observed, and an EPR signal at 1.8589 could be detected immediately. After 1 h, the solution was reduced to dryness, and the residue was triturated with anhydrous ether to yield a green powder, which was filtered, washed with ether, and dried under vacuum. Yield: 114 mg, 95%.

Anal. Calcd for $C_{20}H_{26}B_2F_4N_7OS_2W\cdot 0.25CH_2Cl_2$: C, 32.50; H, 3.57; N, 13.11. Found: C, 32.44; H, 3.57; N, 13.11. IR (KBr): ν(BH) 2565 m, 1595 m, ν(CN) 1543 s, 1449 s, 1417 s, 1386 m, 1352 s, 1281 w, 1209 s, ν(BF_4^-) 1084 s, ν(W═O) 955 s, 859 m, 813 m, 775 m, 727 w, 690 w, 649 m, 476 w, 342 s cm^{-1}. EPR (1/1 CH_2Cl_2/toluene): g_1 1.9125, g_2 1.8604, g_3 1.8115, $\langle g\rangle$ 1.8589.

Table 1. Crystallographic Data

	Tp*WOS(S_2PPh_2)·1/2$C_2H_4Cl_2$	[Tp*WO(pyS_2)]BF_4
formula	$C_{28}H_{34}BClN_6OPS_3W$	$C_{20}H_{26}B_2F_4N_7OS_2W$
formula mass	827.9	726.07
cryst syst	triclinic	monoclinic
space group	$P\bar{1}$	*Cc*
a (Å)	10.732(6)	16.007(5)
b (Å)	16.91(1)	14.091(4)
c (Å)	10.021(4)	13.608(4)
α (deg)	104.40(4)	90
β (deg)	107.52(3)	124.525(4)
γ (deg)	96.09(5)	90
V (Å^3)	1647(1)	2528.8(13)
Z	2	4
ρ_{calcd}, g·cm^{-3}	1.669	1.907
R	0.040	0.054
R_w	0.045	0.118

Table 2. Selected Bond Distances (Å) and Angles (deg) for Tp*WOS(S_2PPh_2-*S*)

W−O(1)	1.712(7)	W−S(1)	2.162(3)
W−S(2)	2.420(2)	W−N(11)	2.285(7)
W−N(21)	2.361(7)	W−N(31)	2.165(7)
S(2)−P(1)	2.086(3)	P(1)−S(3)	1.956(3)
O(1)−W−S(1)	101.5(2)	O(1)−W−S(2)	101.5(2)
O(1)−W−N(11)	88.7(3)	O(1)−W−N(21)	165.9(3)
O(1)−W−N(31)	93.6(3)	S(1)−W−S(2)	98.12(9)
S(1)−W−N(11)	169.8(2)	S(1)−W−N(21)	91.9(2)
S(1)−W−N(31)	96.9(2)	S(2)−W−N(11)	80.6(2)
S(2)−W−N(21)	80.8(2)	S(2)−W−N(31)	156.1(2)
N(11)−W−N(21)	77.9(3)	N(11)−W−N(31)	81.4(3)
N(21)−W−N(31)	80.2(3)	W−S(2)−P(1)	110.1(1)
S(2)−P(1)−S(3)	117.7(2)		

Crystal Structures. Dark orange crystals of Tp*WOS(S_2PPh_2)·1/2$C_2H_4Cl_2$ were grown by slow diffusion of hexane into a saturated 1,2-dichloroethane solution of the complex. A crystal of dimensions 0.07 × 0.18 × 0.24 mm^3 was selected for X-ray analysis. Intensity data were collected at −50 °C on a Rigaku AFC6R diffractometer fitted with Mo Kα radiation. The $\omega-2\theta$ scan technique was used to measure 5817 unique data such that θ_{max} was 25.0°. Corrections were applied for Lorentz and polarization effects,[15] and an empirical absorption correction was applied.[16] The structure was solved by Patterson methods[17] and refined by a full-matrix least-squares procedure based on *F* for 3579 data with $I > 3.0\sigma(I)$.[15] Non-H atoms were refined anisotropically and H atoms included in their calculated positions. Some dynamic disorder was noted in the 1,2-dichloroethane molecule as manifested in relatively large displacement parameters and nonideal bond distances. Crystallographic data are summarized in Table 1, and selected bond distances and angles are presented in Table 2.

Green crystals of [Tp*WO(pyS_2)]BF_4 were grown by slow diffusion of diethyl ether into a dichloromethane solution of the complex. A needle of approximate dimensions 0.08 × 0.10 × 0.40 mm^3 was selected for data collection. Intensity data were collected with a Bruker SMART Apex CCD detector using Mo Kα radiation.[18] Accurate cell parameters and crystal orientation were obtained by least-squares refinement of 4101 reflections with θ values between 2.14° and 21.94°, respectively. Data were reduced

(15) *teXsan: Structure Analysis Software*; Molecular Structure Corporation: The Woodlands, TX.
(16) Walker, N.; Stuart, D. *Acta Crystallogr., Sect. A* **1983**, *39*, 158.
(17) Beurskens, P. T.; Admiraal, G.; Beurskens, G.; Bosman, W. P.; García-Granda, S.; Smits, J. M. M.; Smykalla, C. *The DIRDIF program system*; Technical Report of the Crystallography Laboratory; University of Nijmegen: Nijmegen, The Netherlands, 1992.
(18) *SMART, SAINT and SADABS*; Siemens Analytical X-ray Instruments Inc.: Madison, WI, 1999.

Table 3. Selected Bond Distances (Å) and Angles (deg) for $[Tp^*WO(pyS_2)]BF_4$

W−O(1)	1.632(12)	W−S(1)	2.317(7)
W−N(1)	2.128(15)	W−N(11)	2.235(13)
W−N(21)	2.07(3)	W−N(31)	2.082(16)
S(1)−S(2)	2.037(9)		
O(1)−W−S(1)	100.6(6)	O(1)−W−N(1)	95.2(6)
O(1)−W−N(11)	167.3(6)	O(1)−W−N(21)	87.9(7)
O(1)−W−N(31)	100.4(5)	S(1)−W−N(1)	84.8(4)
S(1)−W−N(11)	90.6(4)	S(1)−W−N(21)	171.5(5)
S(1)−W−N(31)	94.5(5)	N(1)−W−N(11)	79.7(6)
N(1)−W−N(21)	94.4(7)	N(1)−W−N(31)	164.3(7)
N(11)−W−N(21)	81.0(6)	N(11)−W−N(31)	84.6(5)
N(21)−W−N(31)	84.0(8)	W−S(1)−S(2)	96.7(3)
S(1)−S(2)−C(1)	102.4(9)		

using the program SAINT and corrected for absorption (ratio of max/min transmission 0.71).[18] The structure was solved by direct methods and difference Fourier synthesis.[18] Hydrogen atoms were included in calculated positions. Full-matrix least-squares refinement on F^2, using all data, was carried out with anisotropic displacement parameters applied to all non-hydrogen atoms. Crystallographic data are summarized in Table 1, and selected bond distances and angles are presented in Table 3. Figures for both molecular structures were drawn at the 50% probability level using ORTEP.[19]

X-ray Absorption Spectroscopy. Data Collection. X-ray absorption spectroscopy was carried out at the Stanford Synchrotron Radiation Laboratory with the SPEAR storage ring containing 60−100 mA at 3.0 GeV. Tungsten L_{III}-edge spectra were collected on beamline 7-3 using a Si(220) double crystal monochromator with an upstream vertical aperture of 1 mm and a wiggler field of 1.8 T. Harmonic rejection was accomplished by detuning one monochromator crystal to approximately 60% off-peak, and no specular optics were present in the beamline. X-ray absorption was measured in transmittance by using nitrogen-filled ion chambers. The spectrum of a standard tungsten foil was collected simultaneously and the energy calibrated with reference to the lowest energy L_{III}-edge inflection point of the standard which was assumed to be 10207.0 eV. Samples were diluted by grinding with boron nitride so that the maximum absorbance was approximately 2.0 and examined at temperatures of ca. 10 K.

Sulfur K-edge experiments were performed on beamline 6-2 using a Si(111) double crystal monochromator and wiggler field of 1.0 T. Harmonic rejection was accomplished by using a flat nickel coated mirror downstream of the monochromator adjusted so as to have a cutoff energy of about 4500 eV. Incident intensity was monitored using an ion chamber contained in a (flowing) helium-filled flight path. Energy resolution was optimized by decreasing the vertical aperture upstream of the monochromator and quantitatively determined to be 0.51 eV by measuring the width of the 2471.4 eV 1s → $\pi^*(3b_1)$ transition of gaseous SO_2, which corresponds to a transition to a single orbital, rather than to a band of orbitals which can be the case with solid standards.[20] X-ray absorption was monitored by recording total electron yield, and the energy scale was calibrated with reference to the lowest energy peak of the sodium thiosulfate standard ($Na_2S_2O_3 \cdot 5H_2O$) which was assumed to be 2469.2 eV.[21]

Data Analysis. Data were analyzed using the EXAFSPAK suite of computer programs (http://ssrl.slac.stanford.edu/EXAFSPAK.html), and no smoothing or related operations were performed upon the data. The extended X-ray absorption fine structure (EXAFS) oscillations $\chi(k)$ were quantitatively analyzed by curve-fitting using ab initio theoretical phase and amplitude functions calculated using the program FEFF (v. 8.2) of Rehr and coworkers.[22,23] Peak positions in near-edge spectra were estimated by curve-fitting to a sum of pseudo-Voigt peaks using the program EDG_FIT (pseudo-Voigt deconvolution).[24] EXAFS results are presented in Table 4.

Table 4. EXAFS Curve Fitting Results[a]

compd	*N*/W-atom	*R* (Å)	σ^2 (Å^2)	E_0 (eV)	fit error[b]
$Tp^*WOS(S_2PPh_2)$	1 W═O	1.703(1)	0.0016(1)	−17(1)	0.214
	1 W═S	2.142(2)	0.0015(1)		
	1 W−S	2.419(1)	0.0003(1)		
	3 W−N	2.188(5)	0.0059(7)		
Tp*WOS(pyS)	1 W═O	1.706(3)	0.0016(2)	−18(2)	0.335
	1 W═S	2.152(9)	0.0011(5)		
	1 W−S	2.399(5)	0.0019(3)		
	3 W−N	2.17(1)	0.0020(8)		
$[Tp^*WO(pyS_2)]BF_4$	1 W═O	1.690(2)	0.0017(2)	−16(1)	0.308
	1 W−S	2.373(3)	0.0024(2)		
	4 W−N	2.130(4)	0.0055(3)		
	1 W−S	3.274(5)	0.0027(4)		

[a] Coordination number *N*, interatomic distance *R* (Å), and (thermal and static) mean-square deviation in *R* (the Debye−Waller factor) σ^2 (Å^2). The values in parentheses are estimated standard deviations (precisions) obtained from the diagonal elements of the covariance matrix. We note that the accuracies will be somewhat larger than the precisions, typically ±0.02 Å for *R* and ±20% for *N* and σ^2. [b] The fit error is defined as $\sum k^6(\chi_{exptl} - \chi_{calcd})^2/\sum k^6\chi_{exptl}^2$.

Results and Discussion

Oxo−Thio−W(VI) Complexes: Synthesis and Characterization. The reactions of $Tp^*WS(S_2PR_2\text{-}S)(CO)$ (R = OEt, Ph)[11,14] with pyridine *N*-oxide in refluxing toluene gave moderate yields (ca. 50%) of orange, air-stable, *cis*-oxo−thio−W(VI) complexes, $Tp^*WOS(S_2PR_2\text{-}S)$. Other oxygen atom donors (e.g., dimethyl sulfoxide) and solvents could be employed in the reaction but yields were generally lower (10−20%). Alternative syntheses for the phenyl derivative include the reaction of $Tp^*WO(S_2PPh_2)$ with propylene sulfide (ca. 2 days) or elemental sulfur (1 h) in refluxing benzene; the yields of these reactions were ca. 80−90%.[14] The complexes are soluble in chlorinated solvents, tetrahydrofuran, and aromatic hydrocarbons but insoluble in alcohols, acetonitrile, and alkanes.

Microanalytical and mass spectrometric data confirmed the formulations. Peak clusters assignable to $[M - H]^+$ [*m*/*z* 713 (R = OEt), 777 (R = Ph)], $[M - SPR_2]^+$, and $[M - S_2PR_2]^+$ were observed in electron impact mass spectra. The IR spectra of the complexes exhibited ν(W═O) at 931 cm^{-1} and ν(W═S) at 488 cm^{-1} (R = OEt) and 485 cm^{-1} (R = Ph). The ν(W═E) modes are typical of other oxo−thio−W(VI) complexes (E = O, 940−930 cm^{-1}; E = S, ca. 480 cm^{-1}).[10−12,25] An intense band assigned to ν(P═S) was observed at ca. 645 cm^{-1}. The ^{1}H NMR spectra of the complexes displayed resonance patterns indicative of mo-

(19) Johnson, C. K. *ORTEP*; Report ORNL-5138; Oak Ridge National Laboratory: Oak Ridge, TN, 1976.
(20) Song, I.; Rickett, B.; Janavicius, P.; Payer, J. H.; Antonio, M. R. *Nucl. Instrum. Methods* **1995**, *A360*, 634.
(21) Sekiyama, H.; Kosugi, N.; Kuroda, H.; Ohta T. *Bull. Chem. Soc. Jpn.* **1986**, *59*, 575.
(22) Rehr, J. J.; Mustre de Leon. J.; Zabinsky, S. I.; Albers, R. C. *J. Am. Chem. Soc.* **1991**, *113*, 5135.
(23) Mustre de Leon, J.; Rehr, J. J.; Zabinsky, S. I.; Albers, R. C. *J. Phys. Chem.* **1991**, *B44*, 4146.
(24) Pickering, I.; George, G. N. *Inorg. Chem.* **1995**, *34*, 3142.

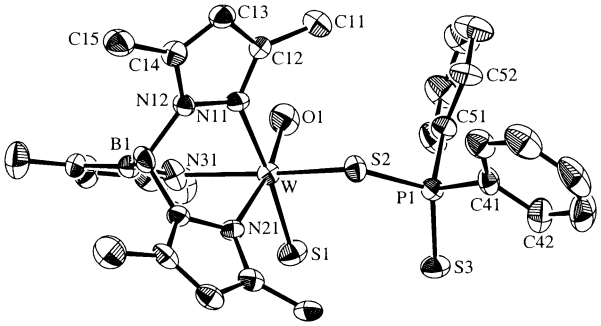

Figure 2. Molecular structure and crystallographic numbering scheme for Tp*WOS(S_2PPh_2-*S*). The numbering schemes of the pyrazole units containing N(21) and N(31) follow that shown for the ring containing N(11).

lecular C_1 symmetry. Typical resonances were observed for the phosphorus containing ligands. $^{31}P\{^1H\}$ NMR spectra displayed a single resonance at δ 67.71 (R = Ph) or δ 121.42 (R = OEt). Resonances in the range δ_P 80−110 have been reported for related Mo complexes.[26] The orange complexes were characterized by strong LMCT bands in the UV region and were devoid of low energy d−d transitions, as expected for formally d^0 complexes.

Reaction of pink Tp*WOSCl with sodium pyridine-2-thiolate and 18-crown-6 in refluxing toluene produced red Tp*W^{VI}OS(pyS-*S*). In contrast, sulfur atom transfer to Tp*Mo^{IV}O(pyS-*N*,*S*) resulted in oxidation of sulfur and the generation of the green (dithio)oxo complex, Tp*Mo^{IV}O-(pyS_2-*N*,*S*).[7] Microanalytical and mass spectrometric (*m*/*z* 639 for $[M]^+$) data confirmed the formulation of Tp*WOS(pyS). The infrared spectrum of the compound revealed bands assignable to ν(W═O) (923 cm^{-1}) and ν(W═S) (480 cm^{-1}) and Tp* and pyS ligands. The ν(W═E) modes are typical of other oxo−thio−W(VI) complexes (vide supra);[10−12,25] in contrast, the ν(Mo═O) band of Tp*MoO(pyS_2) is observed at 960 cm^{-1}.[7] The ^1H NMR spectrum confirmed molecular C_1 symmetry with pyrazolyl methyl resonances in the range δ 2.3−3.0, characteristic of related Tp*WOSX complexes. The spectrum was devoid of the shielded resonance at ca. δ 1.5 observed for Tp*MoO(pyS_2). The red color of the complex was also consistent with an oxo−thio−W(VI) formulation, rather than an alternative (dithio)oxo−W(IV) formulation. The properties of the compound are very similar to those of Tp*WOS(SPh).[12]

Structural Studies. The structure of Tp*WOS(S_2PPh_2)·1/2$C_2H_4Cl_2$ (see Figure 2) was determined by X-ray crystallography, and selected bond distances and angles are presented in Table 2. The triclinic unit cell comprises two complexes and one molecule of 1,2-dichloroethane disposed about a center of inversion. The closest non-H intermolecular contact of 3.37(1) Å occurs between the O(1) and C(35)^i atoms; this corresponds to an O(1)···H^i separation of 2.87 Å (symmetry operation *i*: $-x, -y, -z$). The mononuclear complex is six-coordinate with a distorted octahedral coordination sphere. A *fac* tridentate Tp* ligand and mutually *cis* terminal oxo, terminal thio, and monodentate dithiophosphinate ligands are bonded to the metal center. The W−O(1) and W−S(1) distances of 1.712(7) and 2.162(3) Å, respectively, are within the ranges expected for terminal oxo and thio ligands on W.[10−12,27,28] The W−S(2) distance of 2.420(2) Å is typical of monodentate dithiophosphinate species and close to equivalent bond distances in Tp*-WE(S_2PPh_2-*S*)(CO) (E = O, S).[11,14] The W···S(3) distance of 4.318(3) Å is well outside the sum of the van der Waals radii for the elements (3.8 Å).[29] The S(1)···S(3) distance of 3.266(4) Å is considerable longer than the analogous interactions in Tp*MoOS($S_2PPr^i_2$) (2.396(3) Å)[8] and Tp*-MoOS(S_2PPh_2) (2.383(2) Å),[30] consistent with the absence of any bonding interaction. However, a very weak interaction is indicated by the spatial conjunction of the sulfur atoms and an S(1)···S(3) distance less than the van der Waals distance of 3.7 Å. The O(1)−W−S(1) angle of 101.5(2)° is comparable to corresponding angles in $[WOS(NCS)_4]^{2-}$ (103.3(2)°)[25c] and Tp*WOS{(−)-mentholate} (102.0(6)°).[10−12] The W−N(31) and W−S(2) vectors are inclined away from the terminal chalcogenide ligands with attendant S(2)−W−N(31) and N(11)−W−N(21) angles of 156.1(2)° and 77.9(3)°, respectively. The atoms W, O(1), S(1), N(11), and N(21) are nearly coplanar (mean deviation 0.033 Å, max deviation 0.088(6) Å for O(1)). The W atom lies 0.9410(5) Å out of the plane defined by the O(1), S(1), and S(2) atoms and 1.5198(5) Å out of the plane defined by the N(*n*1) atoms. The W−N(*n*1) distances, W−N(21) > W−N(11) > W−N(31), reflect the relative *trans* influences of the chalcogenido ligands, viz. oxo > thio > dithiophosphinate. The phosphorus atom lies close to the pseudomirror plane defined by the pyrazole ring containing N(31).

Analysis of the W L_{III}-edge EXAFS of Tp*WOS(S_2PPh_2) confirmed the W−ligand distances determined by X-ray diffraction (see Table 4). In support of the oxo−thio−W(VI) formulation, the S K-edge spectrum of Tp*WOS(S_2PPh_2) (Figure 3a) exhibits strong pre-edge features at 2466.4 and 2467.9 eV, along with a prominent peak at 2469.3 eV. The former are characteristic of terminal thio ligation,[12,13] and the latter is characteristic of a "thiolate-like" monodentate

(25) References to other oxo−thio−W(VI) complexes follow. (a) Thiotungstates: Müller, A.; Diemann, E.; Jostes, R.; Bögge, H. *Angew. Chem., Int. Ed. Engl.* **1981**, *20*, 934. (b) WOS(R_2NO)$_2$: McDonell, A. C.; Vasudevan, S. G.; O'Connor, M. J.; Wedd, A. G. *Aust. J. Chem.* **1985**, *38*, 1017. (c) $(PPh_4)_2[WOS(NCS)_4]$: Potvin, C.; Manoli, J. M.; Marzak, S.; Secheresse. F. *Acta Crystallogr., Sect. C* **1988**, *44*, 369. (d) Cp*WOSR (R = Me, CH_2SiMe_3): Faller, J. W.; Ma, Y. *Organometallics* **1989**, *8*, 609. (e) WOSL′(solvent) (L′ = tridentate Schiff base): Yu, S.-B.; Holm, R. H. *Inorg. Chem.* **1989**, *28*, 4385. (f) (L−N_2S_2)WOS (L−N_2S_2 = dianion of *N*,*N*′-dimethyl-*N*,*N*′-bis(2-mercaptophenyl)-1,2-diaminoethane): Barnard, K. R.; Gable, R. W.; Wedd, A. G. *JBIC, J. Biol. Inorg. Chem.* **1997**, *2*, 623. (g) WOS($OSiPh_3$)$_2$(Me_4phen) (Me_4phen = 3,4,7,8-tetramethyl-1,10-phenanthroline): Miao, M.; Willer, M. W.; Holm, R. H. *Inorg. Chem.* **2000**, *39*, 2843.

(26) Young, C. G.; Laughlin, L. J.; Colmanet, S.; Scrofani, S. D. B. *Inorg. Chem.* **1996**, *35*, 5368.

(27) References to bis(thio)−W(VI) complexes follow. (a) Thiotungstates.[25a] (b) $WS_2(R_2NO)_2$.[25b] (c) Cp*WS_2R (R = Me, CH_2SiMe_3).[25d] (d) Cp*WS_2(S^tBu): Kawaguchi, H.; Yamada, K.; Lang, J.-P.; Tatsumi, K. *J. Am. Chem. Soc.* **1997**, *119*, 10346. (e) (L−N_2S_2)WS_2.[25f] (f) WS_2-($OSiPh_3$)$_2$(Me_4phen).[25g]

(28) (a) Orpen, A. G.; Brammer, L.; Allen, F. H.; Kennard, O.; Watson, D. G.; Taylor, R. *J. Chem. Soc., Dalton Trans.* **1989**, S1. (b) Parkin, G. *Prog. Inorg. Chem.* **1998**, *47*, 1.

(29) Abrahamson, H. B.; Freeman, M. L.; Hossain, M. B.; van der Helm, D. *Inorg. Chem.* **1984**, *23*, 2286.

(30) Laughlin, L. J. Ph.D. Dissertation, University of Melbourne, 1993.

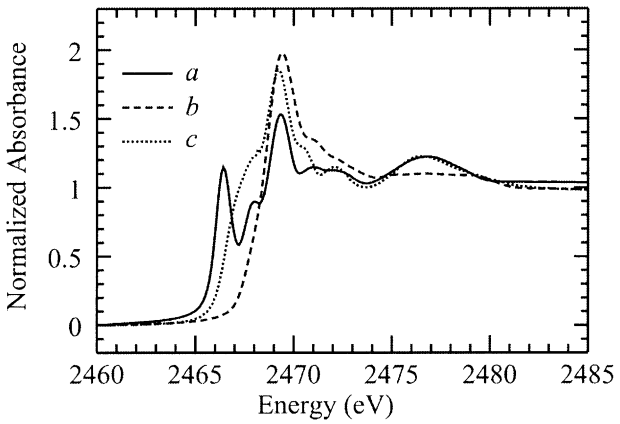

Figure 3. Sulfur K-edge XAS of (a) Tp*WOS(S_2PPh_2), (b) Tp*MoO_2(S_2PPh_2), and (c) Tp*MoOS(S_2PPh_2).

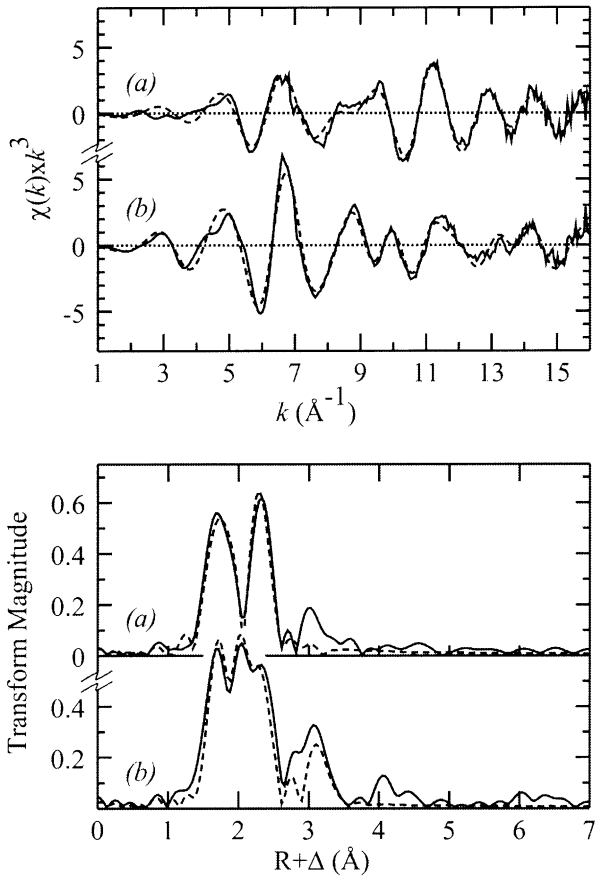

Figure 4. Tungsten L_{III} EXAFS (top), Fourier transforms (bottom), and best fits (- - -) for (a) Tp*WOS(pyS) and (b) [Tp*WO(pyS_2)]BF_4.

$S_2PPh_2^-$ ligand of the type present in Tp*MoO_2(S_2PPh_2)[31] (Figure 3b). A resolved pre-edge feature is not evident in the solid state or solution S K-edge spectra of Tp*MoOS($S_2PPr^i_2$) or Tp*MoOS(S_2PPh_2) (Figure 3c), the spectral signature of the "terminal" Mo═*S*⋯S atom being shifted to higher energy (ca. 2467 eV).

In the absence of single crystals, Tp*WOS(pyS) was structurally characterized using W L_{III}-edge EXAFS (Figure 4a, Table 4) and S K-edge XAS (Figure 5a,b) spectroscopies. Analysis of the W L_{III} EXAFS supported the presence of

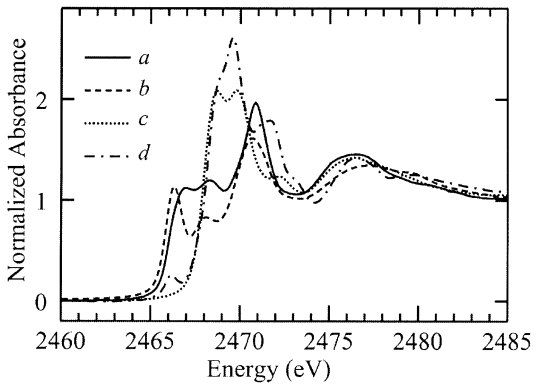

Figure 5. Sulfur K-edge XAS of (a) solid Tp*WOS(pyS), (b) Tp*WOS(pyS) in MeCN solution, (c) Tp*MoO(pyS_2), and (d) [Tp*WO(pyS_2)]BF_4.

terminal oxo, terminal thio, monodentate pyS, and tridentate Tp* ligands. Alternative formulations, e.g., Tp*WOS(pyS-*N*) or Tp*WO(pyS_2), were not compatible with the EXAFS data. For example, a feature due to an "outer-shell" sulfur, as observed in [Tp*WO(pyS_2)]BF_4 (vide infra) and Tp*MoO(pyS_2),[30] was not observed for Tp*WOS(pyS). The unusual "double humped" S K-edge spectrum in Figure 5a was recorded for solid Tp*WOS(pyS); pseudo-Voigt deconvolution of the spectrum reveals at least four transitions at 2466.4, 2467.2, 2468.3, and 2469.6 eV, the lower energy peaks being assigned to the 1s → π^* transitions of a "perturbed" terminal thio ligand. In contrast, the *solution* S K-edge spectrum of Tp*WOS(pyS) exhibits peaks at 2466.3 and 2467.8 eV, indicative of an unperturbed thio ligand (Figure 5b). Interaction of the W═S unit with a pendant pyridine moiety in the solid state would account for these observations. The absence of W⋯W backscattering in the W L_{III} EXAFS of solid Tp*WOS(pyS) argues against intermolecular interactions between thio groups.[13] The S K-edge spectrum of Tp*MoO(pyS_2) (Figure 5c) features transitions typical of disulfides (1s → σ^*_{S-S} and 1s → σ^*_{C-S}) and is devoid of transitions assignable to a terminal thio ligand. The stability of Tp*$Mo^{IV}O(pyS_2$-*N*,*S*) and Tp*W^{VI}OS(pyS-*S*) with respect to their valence isomers, viz., Tp*Mo^{VI}OS(pyS-*S*) and Tp*$W^{IV}O(pyS_2$-*N*,*S*), underscores the relatively facile reduction of thio−Mo(VI) versus thio−W(VI) complexes.

Redox Chemistry. The electrochemical behavior of the complexes in acetonitrile was probed by cyclic voltammetry. The cyclic voltammogram of Tp*WOS(S_2PPh_2) exhibited a quasireversible oxidation at +0.73 V and an irreversible reduction at −0.93 V. Chemical (NBu_4SH or $CoCp_2$) reduction of Tp*WOS(S_2PPh_2) produced unstable [Tp*WOS(S_2PPh_2)]$^-$ (Chart 2), characterized by a broad, highly anisotropic EPR signal (for $CoCp_2^+$ salt: g_1 1.9379, g_2 1.7863, g_3 1.6841, $\langle g\rangle$ 1.8028) typical of oxo−thio−Mo(V)[7,31−33] and −W(V)[25f] anions. Chemical oxidation of Tp*WOS(S_2PPh_2) by $NOBF_4$ initially produced a W-based radical with an EPR signal devoid of ^{31}P coupling ($\langle g\rangle$ 1.8771). This was subsequently replaced by a species that exhibited a doublet EPR signal due to strong ^{31}P coupling

(31) Laughlin, L. J.; Young, C. G. *Inorg. Chem.* **1996**, *35*, 1050.

(32) Xiao, Z.; Bruck, M. A.; Doyle, C.; Enemark, J. H.; Grittini, C.; Gable, R. W.; Wedd, A. G.; Young, C. G. *Inorg. Chem.* **1995**, *34*, 5950.

Chart 2

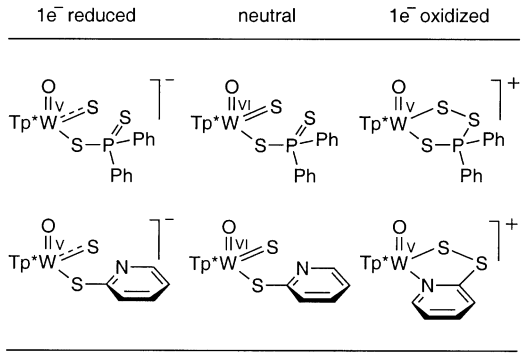

($\langle g \rangle$ 1.8563, A_P 57.0 × 10^{-4} cm^{-1}). These observations are consistent with initial oxidation of the W═S unit followed by internal redox to produce the cationic trithiophosphinate complex in Chart 2. An analogous oxidation is not observed for $Tp^*WO_2(S_2PPh_2)$. In contrast, the cyclic voltammogram of Tp*WOS(pyS) exhibited a reversible reduction at −0.90 V and an irreversible oxidation at +0.56 V. Electrochemical or chemical (NBu_4SH or $CoCp_2$) reduction produced the oxo−thio−W(V) anion, $[Tp^*WOS(pyS)]^-$ (Chart 2), characterized by a highly anisotropic EPR signal (g_1 1.9484, g_2 1.8000, g_3 1.7039, $\langle g \rangle$ 1.8174) typical of anions of this type.[25f] Chemical oxidation of Tp*WOS(pyS) by $NOBF_4$ produced the cationic (dithio)oxo−W(V) species, $[Tp^*WO(pyS_2)]BF_4$ (vide infra). The complex exhibited a strong EPR signal, with $\langle g \rangle$ 1.8589 and a relatively small anisotropy, that confirmed the presence of a pseudoaxial oxo−W(V) species (cf. Mo system[7]). Here, one-electron oxidation of Tp*WOS(pyS) results in a one-electron reduction of W(VI) to W(V) and an overall two-electron S-based oxidation forming a pyridine dithio ligand. This requires disruption of the W−S(py) bond with concomitant S−S bond formation and coordination of the pyridine N to W. These chemical and structural changes are consistent with the irreversible nature of the electrochemical oxidation and the X-ray structure of $[Tp^*WO(pyS_2)]BF_4$ (vide infra).

Isolation and Characterization of a (Dithio)oxo−W(V) Complex. Chemical oxidation of orange Tp*WOS(pyS) using $NOBF_4$ in dichloromethane resulted in the formation of bright green $[Tp^*WO(pyS_2)]BF_4$, which was isolated upon removal of the solvent and trituration with diethyl ether. The color change is consistent with the reduction of W(VI) to W(V) as observed by cyclic voltammetry. The complex was characterized by microanalysis, IR, EPR, and EXAFS spectroscopy, and X-ray crystallography. The presence of a ν(W═O) IR band at 955 cm^{-1}, bands due to BF_4^- (1084 cm^{-1}), and the absence of a band in the region typical of a terminal thio ligand supported the (dithio)oxo−W(V) formulation. The EPR spectra of freshly dissolved samples were identical to the spectra observed from the in situ generated species (vide supra). Tungsten L_{III} EXAFS results (Table 4) were consistent with an (═O)SN_4 coordination sphere and the presence of an S−S bond (inferred from the observation of long-range scattering to sulfur at 3.27 Å). The W K-edge was lower in energy than that of Tp*WOS(pyS), consistent with a formal oxidation state of +V (vs +VI). The S K-edge spectrum was devoid of strong pre-edge features characteristic of terminal thio ligation. A small peak at 2466.2 eV is tentatively ascribed to radiation induced scission of the S−S bond generating an oxo−thio−W(VI) complex containing an N-bound pyridine thionium ligand. The peak is not due to contamination by starting material and does not intensify with successive scans, consistent with rapid reformation of $[Tp^*WO(pyS_2)]^+$ (producing a steady state concentration of the scission product). The X-ray structure of the compound (see Figure 6 and Table 3) revealed a distorted octahedral cation containing facial tridentate Tp*, terminal oxo, and bidentate pyridine-2-dithio-*N*,*S* ligands. The short W−O(1) distance of 1.632(12) Å is typical of oxo−W(V) species, while the W−S(1) (2.317(7) Å) and S(1)−S(2) (2.037(9) Å) distances are those expected for a fully developed singly bonded pyridinedithio−W unit. The "pyridine thiolate" moiety is roughly planar (mean displacement 0.02 Å) but is canted with respect to the W═O vector such that the angle between the plane and vector is 82.8°. Sulfur atom S(1) lies 0.868 Å out of the C_6H_4NS plane, on the side opposite the oxo group, making the chelate ring nonplanar. The W═O vector makes an angle of 74° with the equatorial N_3S plane, being tilted into the region between N(1) and N(21). A lengthening of the W−N bond *trans* to the oxo group is observed. The metrical parameters are totally consistent with the EXAFS analysis summarized in Table 4.

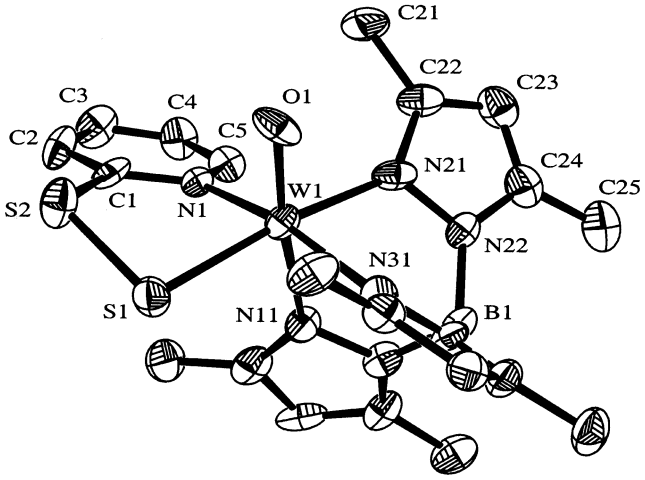

Figure 6. Molecular structure and crystallographic numbering scheme for $[Tp^*WO(pyS_2)]BF_4$. The numbering schemes of the pyrazole units containing N(11) and N(31) follow that shown for the ring containing N(21).

Conclusions

While Mo and W may exhibit similar general chemistries, very stark differences in the behavior of metal−sulfur complexes are emerging. In particular, thio−W(VI) com-

(33) (a) Hinshaw, C. J.; Spence, J. T. *Inorg. Chim. Acta* **1986**, *125*, L17. (b) Dowerah, D.; Spence, J. T.; Singh, R.; Wedd, A. G.; Wilson, G. L.; Farchione, F.; Enemark, J. H.; Kristofzski, J.; Bruck, M. *J. Am. Chem. Soc.* **1987**, *109*, 5655. (c) Wilson, G. L.; Greenwood, R. J.; Pilbrow, J. R.; Spence, J. T.; Wedd, A. G. *J. Am. Chem. Soc.* **1991**, *113*, 6803. (d) Greenwood, R. J.; Wilson, G. L.; Pilbrow, J. R.; Wedd, A. G. *J. Am. Chem. Soc.* **1993**, *115*, 5385. (e) Wedd, A. G., Spence, J. T. *Pure Appl. Chem.* **1990**, *62*, 1055.

plexes are more stable, in terms of metal−ligand redox compatibility, than analogous thio−Mo(VI) species. However, both elements are capable of facile redox interplay with sulfur based co-ligands, especially but not necessarily only upon oxidation. Sulfur-donor co-ligands appear to be especially effective in destabilizing thio−Mo(VI) moieties with respect to valence isomers containing formally reduced Mo centers. The contrasting behavior of Mo/S and W/S systems is a consequence of the very different redox potentials of Mo and W, a factor likely to be important in the disparate biological roles of these elements.

Acknowledgment. We thank Dr. S. D. George and Ms. L. M. R. Hill for running the solution S K-edge spectrum of Tp*WOS(pyS) and Mr. C. J. Doonan for assistance with the electrochemical and EPR experiments. We gratefully acknowledge financial support from the Australian Nuclear Science and Technology Organisation (for travel to SSRL) and the Australian Research Council. SSRL is funded by the Department of Energy (DOE) BES, with further support by DOE OBER and the National Institutes of Health.

Supporting Information Available: Crystallographic data for $Tp^*WOS(S_2PPh_2)\cdot 1/2C_2H_4Cl_2$ (PDF) and $[Tp^*WOS(pyS_2)]BF_4$ (CIF). This material is available free of charge via the Internet at http://pubs.acs.org.

IC030095G